

The Discovery of Primeval Galaxies and the Epoch of Galaxy Formation

Max Pettini

Royal Greenwich Observatory, Madingley Road, Cambridge CB3 0EZ, England

Charles C. Steidel, Kurt L. Adelberger, Melinda Kellogg

Palomar Observatory, Caltech 105–24, Pasadena, CA 91125, USA

Mark Dickinson

Department of Physics and Astronomy, The Johns Hopkins University, Baltimore, MD 21218, USA

Mauro Giavalisco

The Carnegie Observatories, 813 Santa Barbara Street, Pasadena, CA 91101, USA

Abstract.

In the last two years there have been major advances in our ability to identify and study normal star forming galaxies at high redshifts, when the universe was only 15% of its present age. We review the steps which have led to the discovery of a widespread population of objects at $z \sim 3$ with many of the characteristics which we expect for primeval galaxies, and emphasize in particular the advantages of a colour selection technique which targets the Lyman discontinuity at 912 Å.

Star forming galaxies at $z = 3$ resemble local starbursts, although they are typically more luminous by more than one order of magnitude. The ultraviolet continuum is dominated by the integrated light of O and early B type stars and shows prominent interstellar absorption lines which are often blueshifted relative to the systemic velocity of the galaxy, indicating highly energetic outflows in the interstellar medium. Ly α emission is generally weak, probably as a result of resonant scattering. The spectral slope of the ultraviolet continuum and the strength of the H β emission line, which we have detected in a few cases with pilot observations in the infrared K band, suggest that some interstellar dust is already present in these young galaxies and that it attenuates their UV luminosities by a factor of ~ 3 .

The efficiency of our photometric selection technique has allowed us to establish that large scale concentrations of galaxies were already in place at $z = 3$; these structures may be the precursors of today's rich clusters of galaxies, at a time when they were beginning to decouple from the Hubble expansion. In the context of Cold Dark Matter models of structure formation, the galaxies we see must be associated with

very large halos, of mass $M \gtrsim 10^{12} M_{\odot}$, in order to have developed such strong clustering at $z = 3$. We conclude by pointing out the need for infrared space observatories, such as the proposed *Next Generation Space Telescope*, for pushing the quest for the origin of galaxies beyond $z = 5$.

1. Introduction

The quest for the origin of galaxies has been one of the main themes of observational cosmology for many years. A key aspect of this search is the identification of ‘primeval’ galaxies—a somewhat loose concept given that we don’t know how galaxies form, but generally taken to mean the progenitors of galaxies like the Milky Way at the time when they first assembled a significant fraction of their mass and began forming their first generations of stars. Until recently the search for primeval galaxies had been a highly frustrating affair with only a handful of objects, mostly discovered serendipitously or through gravitational lensing, as the meagre return for the investment of many months of observing time on large telescopes.

This, we now realize, was due less to a lack of adequate instrumentation than to the fact that we did not know how to recognise what we were looking for. A typical deep CCD image obtained at the prime focus of a 4 m telescope shows some 3000 galaxies which are at distances stretching from the vicinity of the Milky Way to the most distant reaches of the universe, corresponding to look-back times of 90% of the age of the universe. Thus, such a CCD image in principle contains much of the information required to identify the origin of galaxies and follow their evolution over most of the Hubble time. The challenge until now has been to devise an efficient way to sort this multitude of galaxies according to their redshifts and ages and thereby identify the young counterparts of present day luminous galaxies.

The situation has improved dramatically in the last two years and objects which conform closely to our ideas of a primeval galaxy are now being discovered routinely and in large numbers. In this conference contribution we give an account of these recent exciting developments. We first describe the method which has proved to be most profitable for identifying star forming galaxies at high redshifts. We then review some of the most significant properties of this population of objects, deduced from the analysis of their redshift distribution and their spectra. We end with some comments on future prospects, focussing in particular on the infrared spectral region and on the key role which the *Next Generation Space Telescope* will play in pushing this field of research to the earliest epochs.

Before proceeding just one word of clarification. When dealing with distant galaxies astronomers normally refer to their redshift, because this is the quantity which is directly measured from the spectra. Redshift, however, is only a proxy for look-back time—we are interested in how far in the past we observe a particular galaxy at redshift z . The mapping of redshift to look-back time is not yet as accurate as we would like, although the precision in the measurement of the Hubble constant has improved in the last few years. For reference, Table 1 gives the look-back times corresponding to values of redshift used most often in this

review, adopting a Hubble constant $H_0 = 70 \text{ km s}^{-1} \text{ Mpc}^{-1}$ and a deceleration parameter for the expansion of the universe $q_0 = 0.1$ (unless otherwise stated, these values are assumed throughout this article).

Table 1. Look-Back Time as a Function of Redshift.

z	T (Gyr) ^a	T/T_∞ ^a
0	0	0
0.5	4.6	0.39
1	6.8	0.57
2	8.8	0.74
3	9.8	0.83
4	10.3	0.87
10	11.4	0.96
∞	11.9	1.00

^a $H_0 = 70 \text{ km s}^{-1} \text{ Mpc}^{-1}$; $q_0 = 0.1$

2. Imaging in the Ultraviolet Stellar Continuum

The galaxies we see around us today exhibit a wide variety of shapes and sizes. Approximately half the stars in the present day universe are found in ‘old’ systems, elliptical galaxies and the bulges of spirals, which are collectively referred to as the spheroidal component of the galaxy population. The conventional view has been that these galaxies formed a long time ago, probably before $z = 1$, and relatively rapidly, whereas the assembly of the more fragile disks of spiral galaxies such as the Milky Way was presumably a slower and more protracted process. In this scenario one would expect the formation of ellipticals and bulges to be a period of intense star formation activity.

Star forming galaxies in our vicinity have very characteristic visible spectra. Between 3500 and 7500 Å the spectra are dominated by strong, narrow emission lines of hydrogen, oxygen and nitrogen produced in the nebulae associated with newly formed massive stars. Compared with these strong emission lines the underlying blue continuum radiation from the stars themselves is relatively faint. At redshift $z = 3$ however, the portion of the spectrum recorded by an optical telescope is the rest-frame ultraviolet, between 1000 and 2000 Å. It was only natural that the first searches for galaxies at high redshift should have targeted, either spectroscopically or by narrow-band imaging, what was expected to be the strongest nebular emission line in the ultraviolet, the Ly α line of neutral hydrogen at a rest wavelength of 1215.67 Å. Despite massive efforts, searches for Ly α emission at high redshift have generally been disappointing (e.g. Thompson, Djorgovski, & Trauger 1995). It is only with the benefit of hindsight that we now fully appreciate how difficult it is for Ly α photons to escape the galaxy where they are produced, given the large cross-section for absorption and subsequent

scattering by H I atoms (Meier & Terlevich 1981; Neufeld 1991; Charlot & Fall 1993; Valls-Gabaud 1993).

The method which has turned out to be successful in finding normal galaxies at $z = 3$ was developed by Steidel & Hamilton (1992, 1993) and is based on the realization that the limit of the Lyman series near 912 Å, the wavelength of photons with sufficient energy to ionise hydrogen, produces an obvious discontinuity in the far-UV spectrum of *any* star forming galaxy. This Lyman ‘break’ has a three-fold origin: the intrinsic drop in the spectra of hot O and B type stars which dominate the integrated spectrum at ultraviolet wavelengths (e.g. Cassinelli et al. 1995); the absorption by the neutral interstellar medium within a star forming galaxy (Leitherer et al. 1995a; González Delgado et al. 1997); and the opacity of the intervening intergalactic medium. This last effect, which has been quantified by Madau (1995) from the well known statistics of QSO absorption line spectra, turns out to be the overriding factor which determines the colour of high redshift galaxies.

Steidel & Hamilton devised a three filter system optimised for selecting Lyman break galaxies. Two of the filters, U_n and G in their notation, have passbands respectively below and above the Lyman limit at $z = 3$, while the third filter, \mathcal{R} , is further to the red. In deep images of the sky taken through these three filters $z = 3$ galaxies are readily distinguished from the bulk of lower redshift objects by their red ($U_n - G$) and blue ($G - \mathcal{R}$) colours. As can be seen from Figure 1, high redshift galaxies fall in a well-defined region of the colour-colour plot, irrespective of their spectroscopic type. In the survey which followed the initial observations by Steidel & Hamilton (1992), we designated objects with $(G - \mathcal{R}) < 1.2$ and $(U_n - G) > 1.5 + (G - \mathcal{R})$ (that is with colours within the dotted lines in Figure 1) as ‘robust’ candidates for high redshift galaxies. In order to explore the boundary for high- z galaxies in the two colour plane we also selected a number of ‘marginal’ candidates, defined to be objects with $(G - \mathcal{R}) < 1.2$ and $1.0 + (G - \mathcal{R}) < (U_n - G) < 1.5 + (G - \mathcal{R})$, that is objects falling in a strip half a magnitude wide in $(U_n - G)$ below the sloping line in Figure 1.

Follow-up spectroscopy with the Keck telescopes has confirmed the efficiency of this photometric selection technique (Steidel et al. 1996). Approximately 95% of the robust candidates are indeed high redshift galaxies, the remainder being mainly faint Galactic stars. At the time of this conference (May 1997) we have imaged approximately 800 square arcminutes of sky in a dozen fields. Some of the fields are centred on high redshift QSOs with known intervening Lyman limit systems, while others are random pointings in areas which in some cases have also been imaged with the *Hubble Space Telescope*. At a limiting magnitude $\mathcal{R} \leq 25$, which roughly corresponds to the magnitude of a galaxy like the Milky Way (an L^* galaxy) at $z = 3$, the density of Lyman break galaxies on the plane of the sky is ≈ 0.5 arcmin $^{-2}$ (Steidel, Pettini, & Hamilton 1995), only $\approx 1\%$ of the surface density of *all* galaxies brighter than this limit. Even so, a deep 2048×2048 pixel CCD image recorded at the prime focus of the 5 m Hale telescope at Palomar will yield ~ 40 robust candidates, a vast improvement over the dearth of *bona fide* high redshift galaxies which persisted until a few years ago!

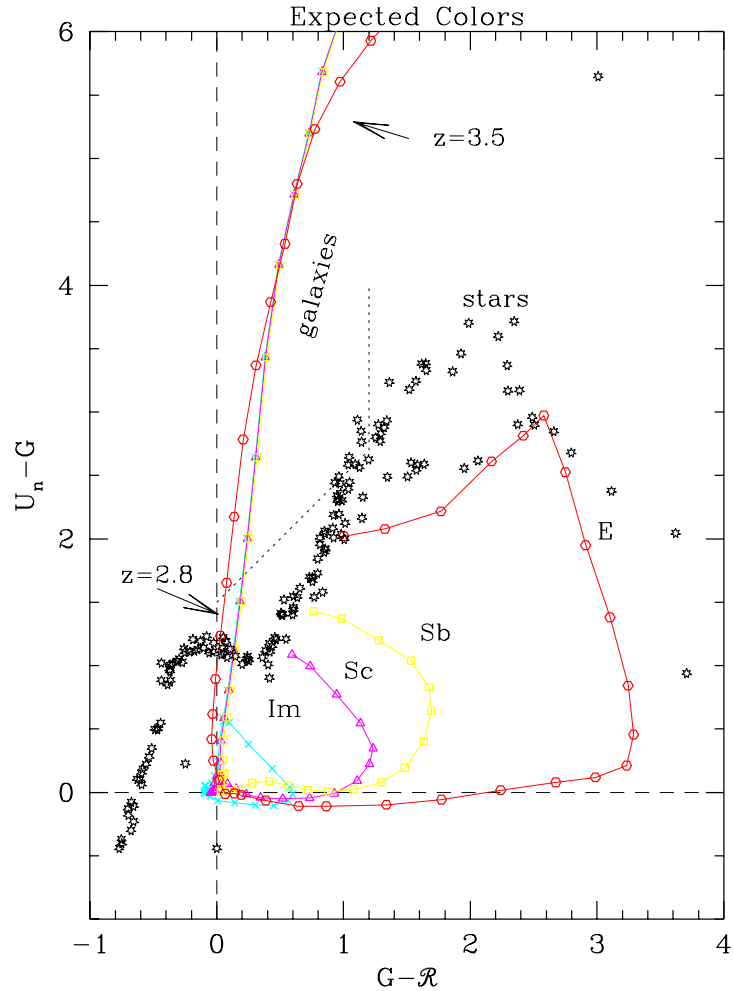


Figure 1. Colour evolution with redshift of galaxies of different spectroscopic type in the U_n , G , \mathcal{R} filter systems devised by Steidel & Hamilton (1993). Magnitudes are defined in the AB system, so that a galaxy with a flat spectrum in f_ν (where f_ν is the flux per frequency unit) has $(U_n - G) = (G - \mathcal{R}) = 0.0$. The curves start at $z = 0$ and each point along a track corresponds to a redshift increment $\Delta z = 0.1$. Colours were calculated from the model spectral energy distributions by Bruzual & Charlot (1996) and Madau's (1995) estimate of the opacity due to Ly α forest and Lyman continuum absorption by intervening gas. The dotted lines indicate the boundary of our photometric selection criteria for robust candidates. The star symbols show the colours of Galactic stars of different spectral type.

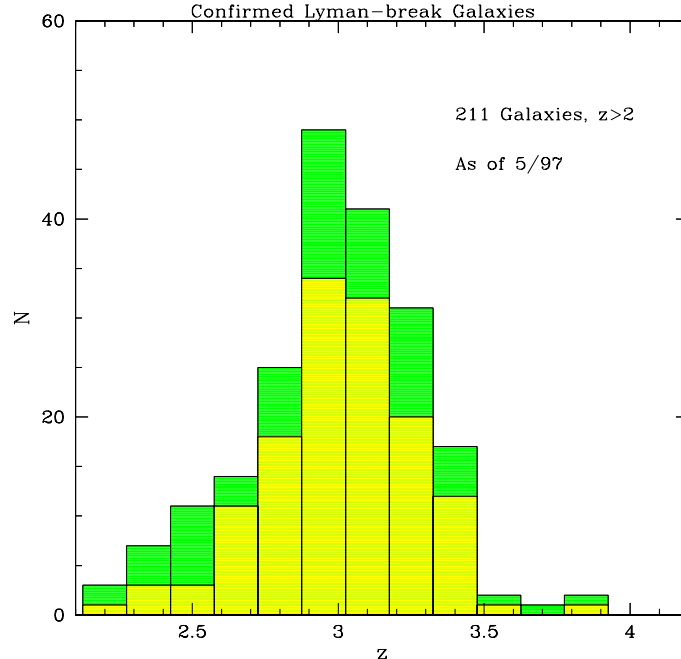


Figure 2. Redshift distribution of spectroscopically confirmed Lyman break galaxies in our survey. The light area refers to the robust candidates only, while the darker area shows the sum of robust and marginal candidates (the corresponding photometric selection criteria are explained in the text).

Figure 2 shows the redshift histogram of all the spectroscopically confirmed galaxies in our sample. Clearly, the U_n , G , \mathcal{R} filter system is most effective at selecting galaxies at redshifts $2.6 < z < 3.4$. As described by Piero Madau (see Figure 4 of his article in this volume) the same Lyman break technique has been applied to the U, B, V, I images of the *Hubble Deep Field* to identify galaxies at redshifts $2.0 < z < 3.4$ (the U drop-outs) and $3.5 < z < 4.5$ (B drop-outs).

3. Large Scale Concentrations of Matter at High Redshift

An immediate bonus of an efficient photometric selection method is the ability to probe with the minimum of effort the three-dimensional distribution of the objects of interest. For Lyman break galaxies at $z \simeq 3$ there is the added advantage that the angular scales sampled map to comoving scales which are sufficiently large to be of interest. This is generally not the case for ‘pencil beam’ surveys at lower redshifts which essentially give a one-dimensional view of clustering along the line of sight. The anisotropy of the cosmic microwave background tells us that seed fluctuations were present at the earliest times; the extent to which these have grown after the first 15% of the age of the universe depends sensitively on the cosmological parameters and can therefore be used to discriminate between different world models.

The first application of the Lyman break technique to the study of large scale structure at high redshift has produced very exciting results and led to

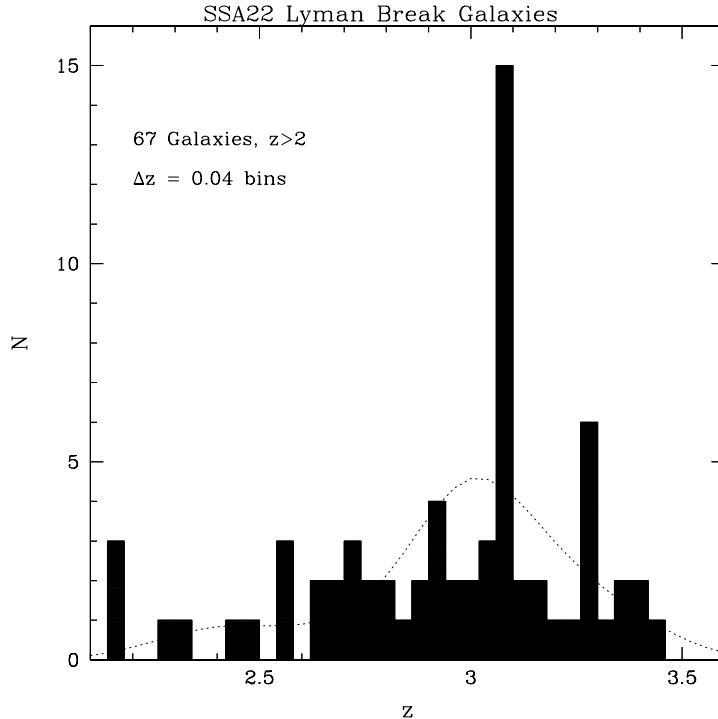


Figure 3. Redshift histogram of all spectroscopically confirmed galaxies in a 9 by 18 arcminute strip of sky near the Hawaii deep field SSA22. The dotted line shows the selection function for our entire survey (normalised to the total number of galaxies in the histogram). The prominent spike at mean redshift $\langle z \rangle = 3.090$ is significant at the 99.8% confidence level.

the discovery of a large concentration of galaxies at $z = 3.090$ in one of our fields (see Figure 3). Our survey suggests that such ‘spikes’ in redshift space were already common at these epochs and may well be examples of today’s rich clusters of galaxies caught early in their evolution, when they were beginning to break away from the Hubble expansion.

One of our best observed regions of sky consists of two adjacent 9×9 arcminute fields which we have imaged very deeply (to a limiting 1σ surface brightness of $29 \text{ mag arcsec}^{-2}$ in all three U_n , G , and \mathcal{R} passbands) with the COSMIC prime focus camera of the 5 m Hale telescope at Palomar Observatory. The strip includes one of the Hawaii deep fields designated SSA22 by Cowie et al. (1996) and overlaps with one of the Canada-France redshift survey fields (Lilly et al. 1995a). We find a total of 181 Lyman break candidates (robust and marginal) brighter than $\mathcal{R} = 25.5$ in this area; their distribution on the plane of the sky is shown in the right-hand panel of Figure 4. Subsequent Keck spectroscopy of a subset of the candidates confirmed that 67 of them are at $z > 2$; of these, 15 galaxies and 1 QSO fall within a redshift interval $\Delta z = 0.04$ centred at $\langle z \rangle = 3.090$. The comoving dimensions of this structure in an Einstein-de Sitter

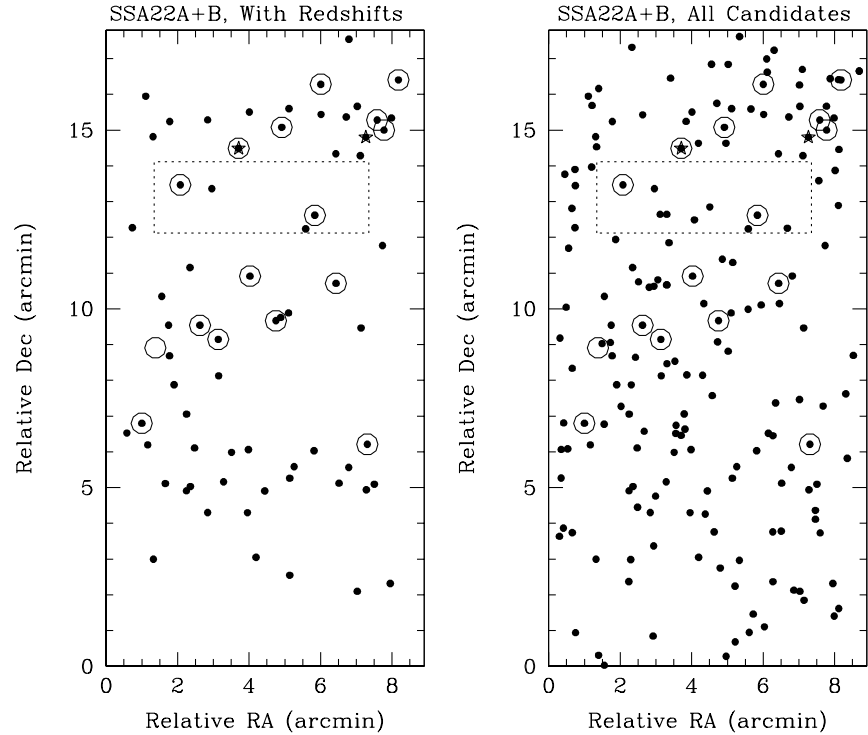


Figure 4. *Left panel:* Distribution on the plane of the sky of all spectroscopically confirmed Lyman break objects with redshift $z > 2$ in the 9×18 arcminute strip. The 16 objects with $\langle z \rangle = 3.090 \pm 0.02$ are circled (the empty circle refers to an object discovered serendipitously from $\text{Ly}\alpha$ emission). The star symbols indicate the two QSOs we found in this field. *Right panel:* All Lyman break candidates in the same area, selected according to both robust and marginal photometric criteria given in the text. The dotted region in both panels shows the Hawaii deep field SSA22 surveyed by Cowie et al. (1996).

universe ($\Omega_M = 1$) are at least $14h_{70}^{-1}$ by $10h_{70}^{-1}$ Mpc in the transverse direction and $16h_{70}^{-1}$ Mpc along the line of sight. On the basis of our sampling frequency we estimate that the concentration contains in excess of 30–50 galaxies brighter than L^* .

The implications of having found such a strong clustering signal at $z = 3$ are considered in detail by Steidel et al. (1997) in the context of Cold Dark Matter theories for the growth of structure in the universe (see David Weinberg’s review at this conference). After correcting for the effect of peculiar velocities, the spike in the redshift histogram corresponds to an overdensity $\delta_r \simeq 2$ relative to the background distribution of mass on the scale of the structure (δ_r is the fractional excess of galaxies which an observer in one of the galaxies in the spike would measure relative to the average of many such volumes). The probability of finding such an overdensity approaches unity only if galaxies are very biased tracers of mass; we deduce values of the bias parameter $b \equiv \delta_{gal}/\delta_{mass} \simeq 2$ for $\Omega_M = 0.2$ and as high as $b \sim 6$ if $\Omega_M = 1$.

In CDM models of galaxy formation (e.g. Baugh et al. 1997) the first galaxies do indeed form in the highest density peaks and a high bias parameter is not unexpected at $z = 3$. Since the more massive halos are more heavily biased (Mo & White 1996), the characteristic mass associated with the Lyman break galaxies can be deduced from the observed bias parameter; the above values of b point to dark halo masses $M \gtrsim 10^{12} M_\odot$. This is strong evidence in support of the view that in the Lyman break objects we see the progenitors of today’s luminous galaxies (L^* and brighter), rather than smaller fragments undergoing an intense and short-lived burst of star formation.

One of the two QSOs we have identified in our observations of the SSA22, at redshift $z_{em} = 3.356$, lies *behind* the concentration of galaxies giving rise to the spike (see Figure 4). It is very interesting to find that the spectrum of this QSO shows absorption systems at the redshifts of the three most significant features in the histogram in Figure 3, $z = 2.93, 3.09,$ and 3.28 . The implication seems to be that diffuse gas with near-unity covering factor is associated with the structures we see in the large scale distribution of galaxies. The combination of absorption and emission techniques will be very powerful for studying the high redshift progenitors of rich clusters of galaxies.

4. The Spectra of High Redshift Galaxies

The sample of more than 200 ultraviolet spectra which we have assembled in our survey is a rich source of information on the physical properties of star forming galaxies at high redshift. The spectra show many similarities with those of nearby starburst galaxies; accordingly our analysis draws extensively on the detailed studies of local starbursts carried out with the *HST* and described in Tim Heckman’s article in this volume. Here we focus in particular on: (a) the UV luminosities and implied star formation rates; (b) evidence for the presence of dust and the corresponding UV extinction; and (c) Ly α emission and large-scale velocity fields in the interstellar medium. The signal-to-noise ratio of most of our spectra, although relatively modest, is nevertheless adequate for addressing all three topics. In addition, we have begun to study in detail a number of individual objects (generally among the more luminous in the sample) to which

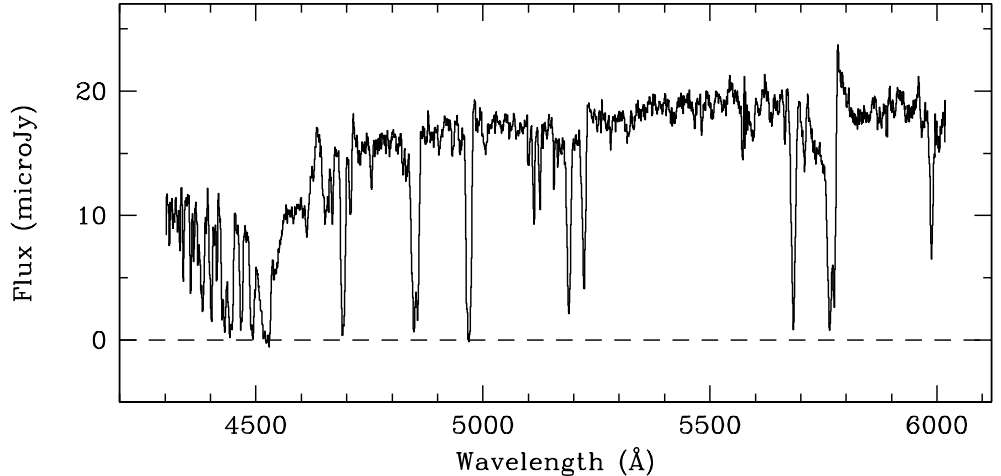


Figure 5. Spectrum of the $V = 20.64$, $z = 2.723$ galaxy 1512-cB58 obtained with LRIS on the Keck I telescope in May and August 1996. With a total exposure time of 11 400 s we reached $S/N \simeq 50$ per pixel at a resolution of 3.5 \AA .

we have devoted long exposure times at moderately high spectral resolution. The best case is the $z = 2.723$ galaxy 1512-cB58 (Yee et al. 1996). This spectrum (reproduced in Figure 5) is of comparable quality with the best *HST* spectra of local starburst galaxies and is a veritable mine of information. It now seems highly likely that cB58, which is ~ 4 magnitudes brighter than the typical $z = 3$ galaxy in our survey, is not extraordinarily luminous but gravitationally lensed (Williams & Lewis 1997; Seitz et al. 1997) and therefore presumably provides us with an unusually clear view of a normal galaxy at high redshift.

4.1. Ultraviolet Luminosities

The typical high- z galaxy in our survey, with $\mathcal{R} = 24.5$, $(G - \mathcal{R}) = 0.5$, and $z = 3$, has a far-UV luminosity $L_{1500} = 1.3 \times 10^{41} h_{70}^{-2} \text{ erg s}^{-1} \text{ \AA}^{-1}$ at 1500 \AA . It is instructive to compare this value with those measured in nearby starbursts. The UV luminosities we find at $z = 3$ are ≈ 800 times greater than that of the brightest star cluster in the irregular galaxy NGC 4214 studied with *HST* by Leitherer et al. (1996), and exceed by a factor of ≈ 30 that of the most luminous local example, the Wolf-Rayet galaxy NGC 1741 which contains $\approx 10^4$ O type stars (Conti, Leitherer, & Vacca 1996).

The ultraviolet spectra, in which we see the integrated continuum of O and early B stars, can in principle be used to estimate the star formation rate in a more direct way than the Balmer lines, which are produced by the reprocessed ionizing radiation of the stars at the very tip of the IMF. Adopting a continuous star formation model with an age greater than 10^8 years and a Salpeter IMF from 0.1 to $100 M_{\odot}$ (Bruzual & Charlot 1996; Leitherer, Robert, & Heckman

1995b), the typical $L_{1500} = 1.3 \times 10^{41} h_{70}^{-2} \text{ erg s}^{-1} \text{ \AA}^{-1}$ corresponds to a star formation rate $SFR \simeq 8 h_{70}^{-2} M_{\odot} \text{ yr}^{-1}$. This is probably a lower limit, since dust extinction (see below) and a lower age would both raise this value (for an age of 10^7 years the implied SFR is greater by a factor of ≈ 1.7).

It is interesting to note that even the brightest objects in our sample fall well within the surface brightness distribution of local starbursts. The highest values of L_{1500} which we have found are $\sim 4\text{--}5$ times higher than the median. Adopting a typical extinction correction of a factor of ≈ 3 at 1500 \AA (see below) and a typical half-light radius $r \simeq 2 \text{ kpc}$ (Giavalisco, Steidel, & Macchetto 1996), we arrive at a star formation intensity (SFR per unit area) $\dot{\Sigma} \sim 13 M_{\odot} \text{ yr}^{-1} \text{ kpc}^{-2}$. This value compares well with the upper envelope of the ultraviolet sample considered by Meurer et al. (1997). Thus, the star forming galaxies which we are finding at high redshift appear to be spatially more extended versions of the local starburst phenomenon. The same physical processes which limit the maximum star formation intensity in nearby starbursts, as discussed by Meurer et al., also seem to be at play in young galaxies at high redshift which may well be undergoing their first episodes of star formation.

4.2. Dust Extinction

Dust is a ubiquitous component of the interstellar medium; given that galaxies at $z = 3$ are obviously already enriched in heavy elements, it is likely that some dust is mixed with the gas and stars we observe. Unfortunately, even relatively small amounts of dust can have a significant effect in the rest-frame ultraviolet and thereby alter our view of high- z galaxies. In particular, dust will: (a) extinguish resonantly scattered emission lines, most notably $\text{Ly}\alpha$; (b) attenuate the UV continuum leading to underestimates of the star formation rate; and (c) redden the broad spectral energy distribution so that it resembles that of an older stellar population. To some extent we have to learn to live with these problems because of the inherent uncertainties of any dust corrections which arise mostly from the unknown shape of the extinction law.

The intrinsic slope of the integrated UV continuum of a star forming galaxy is a robust quantity which, as explained for example by Calzetti (1997a), varies little with the exact shape of the IMF or the age of the starburst. Spectral synthesis models show that the continuum between 1200 and 1800 \AA is well approximated by a power law of the form $f_{\nu} \propto \lambda^{\alpha}$ with α between -0.5 and 0 . Similarly, the empirical template starburst spectrum constructed by Calzetti (1997b) has $\alpha = -0.1$. In contrast, the galaxies we observe generally have UV spectral slopes between 0 and $+1.5$; the spectrum of cB58 reproduced in Figure 5, for example, can be clearly seen to be redder than flat spectrum and has $\alpha = +1.3$. Such (relatively) red spectra can result from an aging starburst or from an IMF lacking in massive stars, but we regard both possibilities as unlikely because with sufficiently high S/N we see directly the spectral signatures of O stars. The most straightforward interpretation, in analogy with local starbursts, is that the spectra are reddened by dust extinction.

In Figure 6, reproduced from Dickinson et al. (1997), we use the $(G - \mathcal{R})$ colours of the entire sample of spectroscopically confirmed galaxies to estimate dust corrections to the star formation rates at high redshift. Assuming an intrinsic spectral slope $\alpha = -0.13$, as is the case for a Bruzual & Charlot (1996)

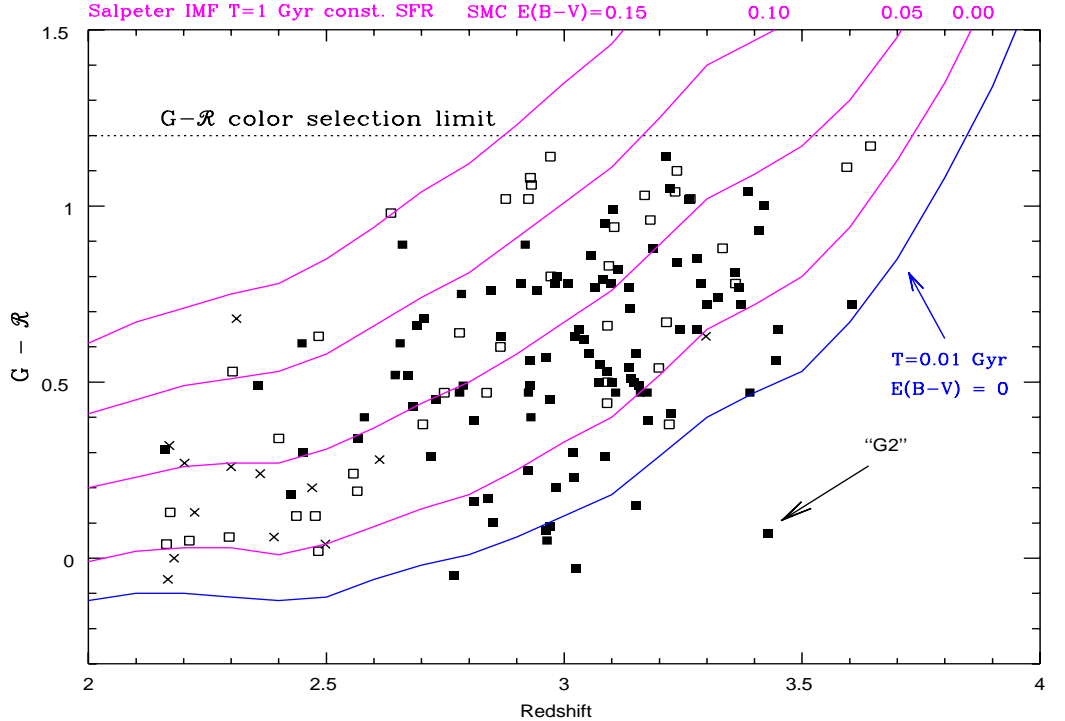


Figure 6. Comparison between observed and predicted ($G - \mathcal{R}$) colours of Lyman break galaxies for different amounts of SMC-type ultraviolet extinction and for different ages of the stellar populations. The symbols correspond to different photometric selection criteria, but all the galaxies plotted here have spectroscopically confirmed redshifts.

model with 1 Gyr old continuous star formation and Salpeter IMF, the curves labelled with different values of $E(B - V)$ at the top of the figure show the predicted ($G - \mathcal{R}$) colour as a function of redshift, if the spectra of high- z galaxies are reddened with an extinction law similar to that which applies to stars in the Small Magellanic Cloud. The curves all rise to redder ($G - \mathcal{R}$) colour with redshift due to the increasing line blanketing by the Ly α forest (Madau 1995).

The difference between the observed and predicted ($G - \mathcal{R}$) colour yields the extinction at 1500 Å, A_{1500} , appropriate to each galaxy; by adding together the individual values for all the galaxies in the sample Dickinson et al. (1997) deduce a net correction by a factor of 1.8 to the comoving volume-averaged star formation rate (in $M_{\odot} \text{ yr}^{-1} \text{ Mpc}^{-3}$) at $z = 3$. Using the greyer extinction law deduced by Calzetti, Kinney, & Storchi-Bergmann (1994) from the integrated spectra of nearby starbursts increases the net correction to a factor of 3.5. Also shown in Figure 6 is the zero-reddening curve for a younger stellar population (10 Myr) which has a bluer intrinsic UV slope $\alpha = -0.42$ (Bruzual & Charlot 1996). If the models are correct, some of the galaxies we have found are evidently younger than 10^9 years, since they lie between the two zero-reddening curves in

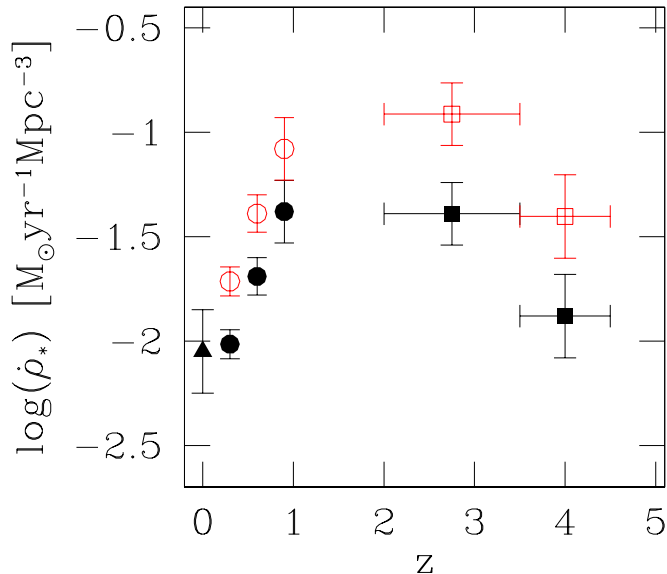


Figure 7. The comoving volume-averaged star formation rate as a function of redshift, reproduced from Madau (1997) for $H_0 = 50 \text{ km s}^{-1}$ and $q_0 = 0.5$. The filled squares are measurements from the *HDF*, the circles from the *Canada-France Redshift Survey* and the triangle from a local $\text{H}\alpha$ survey. The open symbols show the same values corrected for dust extinction.

Figure 6.¹ Adopting the 10^7 year model as the unreddened template leads to corrections to the global star formation rate by factors of 3.5 and 6.3, for the SMC and Calzetti et al. extinction laws respectively. However, we consider it very unlikely that *most* Lyman break galaxies are $\sim 10^7$ year old bursts, given that their number density and their masses are roughly comparable to those of present day L^* galaxies (Steidel et al. 1995, 1997).

We conclude that the likely dust correction to the integrated ultraviolet luminosity of Lyman break galaxies at $z = 3$ amounts to a factor of ~ 3 . The correction could be as low as ~ 2 and as high as ~ 6 , depending on the age of the stellar population and on the wavelength dependence of the ultraviolet extinction. As discussed in section 5 below, in the few cases where we have detected the redshifted $\text{H}\beta$ emission line in Lyman break galaxies, the line flux we measure confirms the relatively low values of ultraviolet extinction deduced by Dickinson et al. (1997).

¹There are a few points with $(G - \mathcal{R})$ colours *bluer* than the 10^7 year curve in Figure 6. $\text{Ly}\alpha$ emission line contamination may play a role for some, particularly for the most deviant object labelled “G2” which is an AGN with strong line emission. Differences by $\lesssim 0.1$ mag can easily be explained by photometric errors and the stochastic nature of the $\text{Ly}\alpha$ forest blanketing.

The open squares in Figure 7 show the effect of a factor of 3 correction for dust extinction on the comoving volume-averaged star formation rate deduced by Madau (1997) from the density of U and B drop-outs in the *Hubble Deep Field*. Given that the uncorrected value of $\dot{\rho}_*$ at any epoch deviates by only a factor of ~ 3 from the average over the Hubble time, the inclusion of dust clearly has a significant impact on the interpretation of the cosmic star formation history. The plot in Figure 7 is generally taken to indicate a peak in star formation between $z \sim 1$ and ~ 2.5 . This conclusion probably still holds once dust is taken into account, although the corrections appropriate to galaxies in the *CFRS* (Lilly et al. 1995b) have yet to be determined. Since the values of $\dot{\rho}_*$ from the *CFRS* survey are based on galaxy luminosities in the near-UV (2800 Å), the same amount of dust as we deduced for the Lyman break galaxies would result in an upward correction by a factor of ~ 2 (open circles in Figure 7). A UV dust extinction of ~ 1 mag is supported by the very recent comparison between $H\alpha$ and UV continuum luminosities of *CFRS* galaxies at $z \leq 0.3$ by Tresse & Maddox (1997). The revisions we propose to Madau's plot bring the observed values of $\dot{\rho}_*$ in better agreement with recent theoretical predictions based on CDM models of galaxy formation (see Figure 16 of Baugh et al. 1997).

4.3. Ly α Emission

The Ly α emission line is detected in about 75% of the galaxies in our sample but is always weaker than expected on the basis of the UV continuum luminosities, in agreement with the generally null results of previous searches for high redshift galaxies based on this spectral feature (e.g. Thompson et al. 1995). There are strong indications that the main reason for the weakness of Ly α emission is resonant scattering in an outflowing interstellar medium. When detected, the emission line is generally redshifted by up to several hundred km s $^{-1}$ relative to the interstellar absorption lines and, in the best observed cases, its profile is clearly asymmetric.

The bright galaxy 0000-D6, reproduced in Figure 8, is a good example. The zero point of the velocity scale in Figure 8 is at $z = 2.960$, the redshift of the strong interstellar absorption lines in 0000-D6. On this scale the peak of Ly α emission is at a relative velocity of 800 km s $^{-1}$, and while the red wing extends to ~ 1500 km s $^{-1}$, the blue wing is sharply absorbed. This P Cygni-type profile can be understood as originating in an expanding envelope around the H II region; the unabsorbed Ly α photons we see are those back-scattered from the receding part of the nebula. In agreement with this picture, we find that the systemic velocity of the star-forming region is ≈ 400 km s $^{-1}$, as measured from the wavelengths of weak photospheric lines from O stars (S V $\lambda 1501.96$ and O IV $\lambda 1343.35$), which can be discerned in this high S/N spectrum, and of [O III] $\lambda 5007$ which we have detected in the K -band (see §5 below). Taken together, the relative velocities of interstellar, stellar and nebular lines point to large scale outflows in the interstellar medium, presumably as a consequence of the starburst activity which in this galaxy, one of the brightest in our sample, approaches $\approx 100 h_{70}^{-2} M_{\odot} \text{ yr}^{-1}$. Similar, although generally less energetic, outflows are seen in local starburst galaxies observed with *HST* and *HUT* (Kunth et al. 1996; González Delgado et al. 1997).

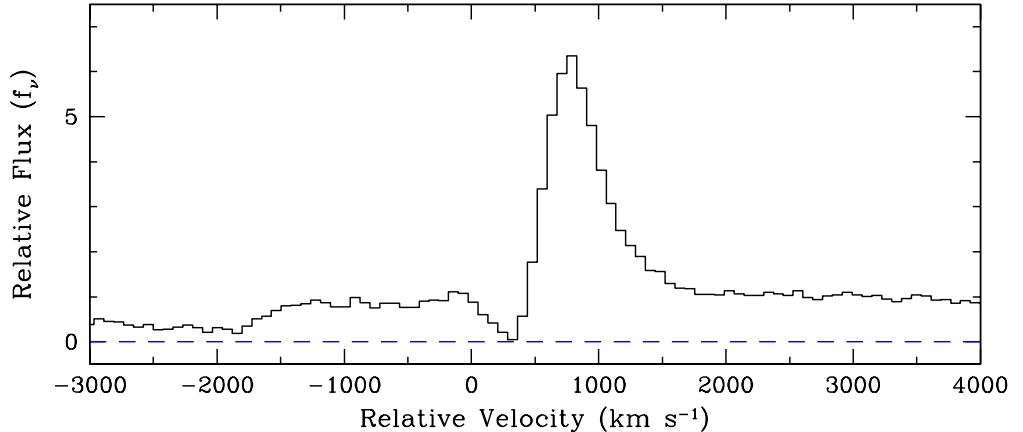


Figure 8. The wavelength region near $\text{Ly}\alpha$ in the $\mathcal{R} = 22.9$, $z = 2.963$ galaxy 0000-D6. The spectrum was obtained with LRIS on Keck I by Hy Spinrad and Arjun Dey with an exposure time of 17 650 s and a resolution of 4 \AA FWHM. The equivalent width of the combined $\text{Ly}\alpha$ emission and absorption feature is 10.5 \AA . The velocity scale is relative to the redshift of the strongest interstellar absorption lines.

Large scale motions of the type we have found in 0000-D6 could be the main reason for the strengths of the interstellar absorption lines in high- z galaxies which, with typical equivalent widths of $2\text{-}3 \text{ \AA}$, are often greater than their counterparts in nearby starbursts. (Since these lines are saturated, their equivalent widths are much more sensitive to the velocity dispersion of the gas than to the metallicity of the gas). On the other hand, such strong absorption lines are also often seen in damped $\text{Ly}\alpha$ systems, which are not generally associated with sites of active star formation and where they may reflect the complex velocity fields of merging protogalactic clumps (Haehnelt, Steinmetz, & Rauch 1997).

In any case, the systemic redshift of $\text{Ly}\alpha$ emission relative to interstellar absorption *along the same sight-line* brings into question the validity of interpreting such differences along adjacent sight-lines as evidence for large rotating disks, as recently proposed by Djorgovski et al. (1996), and Lu, Sargent, & Barlow (1997).

5. Infrared Prospects

At $z \sim 3$ the nebular emission lines which dominate the optical spectra of star forming galaxies are redshifted into the infrared H and K bands; there is a strong incentive to detect and measure these lines as they hold important clues to the nature of the population of high- z galaxies we have isolated. In particular: (a) the line widths, which presumably reflect the overall kinematics of the star forming regions in a galaxy, can provide an indication of the masses involved; (b) a detection of $\text{H}\beta$ (or $\text{H}\alpha$ at $z \lesssim 2.5$) would give a measure of the star formation

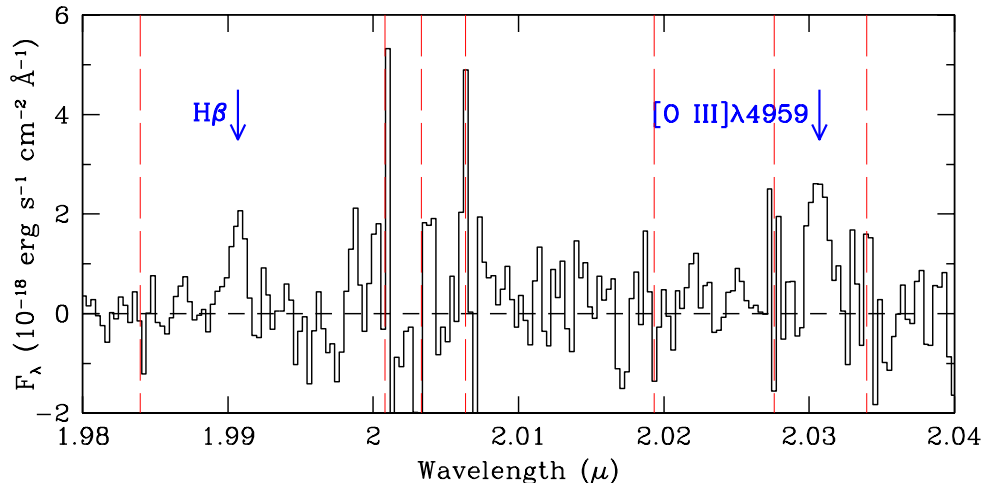


Figure 9. Portion of the infrared spectrum of the $\mathcal{R} = 23.9$, $z = 3.059$ galaxy 0201-C6 obtained with CGS4 on UKIRT in September 1996. The exposure time was 18 000 s and the resolution is 8 \AA FWHM sampled with 2.7 wavelength bins, each 3 \AA wide. The vertical dashed lines indicate the locations of the major OH^- sky emission lines.

rate which can be compared with that deduced from the UV continuum; and (c) the ratios of the familiar nebular lines are probably the most promising way of estimating the metallicity of these galaxies, given the complexity of the ultraviolet absorption line spectra.

Somewhat paradoxically (given that the discovery of $z \sim 3$ galaxies awaited the availability of large telescopes) the detection of the strongest rest-frame optical emission lines in the K -band is actually within reach of 4-m telescopes equipped with moderately high dispersion near-infrared spectrographs. What is required is prior knowledge of the galaxy redshift and sufficient spectral resolution to ensure that the lines of interest fall in a gap between the much stronger OH^- emission features which dominate the infrared sky. Pilot observations which we carried out with the CGS4 spectrograph on UKIRT in September 1996 were successful in detecting $\text{H}\beta$ and/or $[\text{O III}]$ emission lines in both $z \simeq 3$ galaxies targeted, 0000-D6 and 0201-C6; a third measurement—in cB58—has been obtained by Gillian Wright (private communication). Figure 9 shows a portion of the K -band spectrum of 0201-C6. $\text{H}\beta$ and the weaker member $[\text{O III}]$ doublet are both detected at the $\sim 5\sigma$ level, whereas the stronger $[\text{O III}]$ line is lost in the nearby sky emission.

As can be seen from Figure 9, both $\text{H}\beta$ and $[\text{O III}]$ emission lines are resolved; after correcting for the instrumental resolution, we measure $\sigma = 70 \pm 20 \text{ km s}^{-1}$. A similar velocity dispersion is also found in the other two cases, 0000-D6 and cB58. (Incidentally, the fact that cB58 shows the same velocity dispersion as the other two $z \simeq 3$ galaxies, even though it is $\gtrsim 10$ times brighter,

is another indication of its gravitationally lensed nature). If we combine $\sigma = 70 \text{ km s}^{-1}$ with the half-light radii of $\approx 2 \text{ kpc}$ deduced for both 0201-C6 and 0000-D6 from *HST* WFPC2 images, we obtain virial masses of $\sim 1.2 \times 10^{10} M_{\odot}$. This is comparable to the mass of the Milky Way bulge (Dwek et al. 1995) and to the dynamical mass within the central $r = 2 \text{ kpc}$ of an L^* elliptical galaxy. However, the total masses involved are likely to be substantially greater, given that the present IR observations sample only the innermost cores of the galaxies, where the star formation rates are presumably highest. As we discussed in §3 above, the clustering properties of Lyman break galaxies strongly suggest that they are associated with dark matter halos of mass $M \gtrsim 10^{12} M_{\odot}$.

The $\text{H}\beta$ flux of 0201-C6 (Figure 9), $(2.6 \pm 0.6) \times 10^{-17} \text{ erg s}^{-1} \text{ cm}^{-2}$, corresponds to a luminosity $L_{\text{H}\beta} = (2.3 \pm 0.5) \times 10^{42} h_{70}^{-2} \text{ erg s}^{-1}$. Adopting an $\text{H}\alpha/\text{H}\beta$ ratio of 2.75 and Kennicutt's (1983) calibration $SFR (M_{\odot} \text{ yr}^{-1}) = L_{\text{H}\alpha} (\text{erg s}^{-1}) / 1.12 \times 10^{41}$ which is appropriate for a Salpeter IMF from 0.1 to $100 M_{\odot}$, we deduce a star formation rate $SFR_{\text{H}\beta} = (55 \pm 13) h_{70}^{-2} M_{\odot} \text{ yr}^{-1}$. For comparison $SFR_{\text{UV}} = (20 - 35) h_{70}^{-2} M_{\odot} \text{ yr}^{-1}$, depending on whether the age of the starburst is 10^9 or 10^7 years respectively. Estimates of the star formation rate from $\text{H}\alpha$ emission and the UV continuum do not normally agree to better than a factor of ~ 2 in local starbursts (e.g. Meurer et al. 1995); the agreement in 0201-C6 is further improved when account is taken of the small amount of reddening ($E(B - V) \lesssim 0.1$) implied by the slope of the UV continuum ($\alpha = 0.35$) using the prescription by Calzetti (1997a). We reach similar conclusions in 0000-D6 and cB58; in all three cases ultraviolet extinctions by factors of $\approx 2 - 3$ are indicated by the comparison between UV and $\text{H}\beta$ luminosities.

These preliminary results demonstrate clearly the great potential of the infrared spectral region for complementing the information provided by the rest-frame ultraviolet and ultimately leading to a better understanding of the nature of high- z galaxies. With large telescopes the detection of nebular emission lines in the near-IR will be easier and it will be possible to address the points touched upon here in greater depth, using a large set of measurements. On the other hand, the strong sky background will remain a fundamental limitation of ground-based observations and will be fully overcome only with space observatories such as the *NGST*. There is therefore a strong motivation to provide *NGST* with at least a moderately high spectral resolution capability ($R \geq 3000$), adequate to resolve the emission lines from star forming galaxies. Free from the complications introduced by the Earth's atmosphere, *NGST* will be able to record the full complement of nebular emission lines and obtain reliable estimates of the abundances of several elements. By bringing together abundance measurements from emission and absorption (Lu et al. 1996; Pettini et al. 1997) line data it will be possible to build a full picture of the early stages in the chemical enrichment history of the universe.

6. Epilogue

Star forming galaxies with spectra broadly similar to those of present day starbursts have now been detected up to redshift $z \simeq 5$ (Franx et al. 1997). It is remarkable that at such an early epoch, only 1.5 Gyr after the Big Bang, many of the characteristics of the present day universe were already in place. The

intergalactic medium was fully ionised, galaxies were enriched in a wide variety of chemical elements (albeit in lower proportions than today), and structures on the scale of rich clusters were already evident. As we learn more about the time when the luminous galaxies of today were beginning to form, already the next goal in our ‘*ORIGINS*’ quest is coming into focus: identifying the time when the first stars formed, produced the first generation of heavy elements and ionised the universe which had remained neutral since the cosmic microwave background was emitted at $z = 1000$.

Our first steps in this unfamiliar territory are guided, as it is often the case, by theoretical considerations. The lowest metallicities measured at $z = 4 - 5$ are $\sim 1/300$ of solar (Pettini et al. 1995; Lu et al. 1996). As discussed by Madau & Shull (1996) and Miralda-Escudé & Rees (1997), the ionising photons associated with the production of even such trace amounts of heavy elements outnumber the baryons by 10 to 1 (this is a rather straightforward calculation, because the same massive stars are the source of heavy elements and ionising photons). Thus, if this initial enrichment took place when the universe was mainly neutral, the associated Lyman continuum radiation was sufficient to reionise all the diffuse gas.

Recently Miralda-Escudé & Rees (1997) and Rees & Miralda-Escudé (1997) have explored some of the consequences of this scenario. They point out that the physics of the galaxy formation process is different depending on whether galaxies form by accreting neutral or photoionised gas, mainly because the cooling efficiency is different in the two cases. They speculate that the first objects to collapse during the ‘dark ages’ of the universe are likely to be on very small scales, with velocity dispersions $\sigma \lesssim 10 \text{ km s}^{-1}$ and masses $M_b \lesssim 10^8 M_\odot$. Under these circumstances the brightest sources at very high redshifts are likely to be Type II supernovae. At $z = 10$ such Population III supernovae may reach an infrared magnitude $K \simeq 30$ and may be as numerous as one supernova per square arcminute per year. While it is just conceivable that an event of this kind may be within reach of current instrumentation if gravitationally lensed by a foreground cluster of galaxies, testing these bold new ideas will be the mission of the *Next Generation Space Telescope*.

References

- Baugh, C.M., Cole, S., Frenk, C.S., & Lacey C.G. 1997, ApJ, in press (astro-ph/9703111)
- Bruzual, G. & Charlot, S. 1996, private communication
- Calzetti, D. 1997a, in *The Ultraviolet Universe at Low and High Redshift*, ed. W. Waller, (Woodbury: AIP Press), in press (1997).
- Calzetti, D. 1997b, AJ, 113, 162
- Calzetti, D., Kinney, A.L., & Storchi-Bergmann, T. 1994, ApJ, 429, 582
- Cassinelli, J.P. et al. 1995, ApJ, 438, 932
- Charlot, S., & Fall, S.M. 1993, ApJ, 415, 580
- Conti, P. S., Leitherer, C., & Vacca, W. D. 1996, ApJ, 461, L87
- Cowie, L.L., Songaila, A., Hu, E.M., & Cohen, J.G. 1996, AJ, 112, 839

- Dickinson, M., et al. 1997, in preparation
- Djorgovski, S.G., Pahre, M.A., Bechtold, J., & Elston, R. 1996, *Nature*, 382, 234
- Dwek, E., et al. 1995, *ApJ*, 445, 716
- Franx, M., Illingworth, G.D., Kelson, D.D., van Dokkum, P.G., & Tran, K-V. 1997, *ApJ*, submitted (astro-ph/9704090)
- Giavalisco, M., Steidel, C.C., & Macchetto, F.D. 1996, *ApJ*, 470, 189
- González Delgado, R., Leitherer, C., Heckman, T.M., Lowenthal, J.D., Ferguson, H.C., & Robert, C. 1997, *ApJ*, submitted
- Haehnelt, M.G., Steinmetz, M., & Rauch, M. 1997, *ApJ*, submitted (astro-ph/9706201)
- Kennicutt, R.C. 1983, *ApJ*, 272, 54
- Kunth, D., Lequeux, J., Mas-Hesse, J.M., Terlevich, E., & Terlevich, R. 1997, in *Starburst Activity in Galaxies*, *Rev. Mex. Astron. Astrofis. Conf. Series*, in press (astro-ph/9612043)
- Leitherer, C., Ferguson, H.C., Heckman, T.M., & Lowenthal, J.D. 1995a, *ApJ*, 454, L19
- Leitherer, C., Robert, C., & Heckman, T.M. 1995b, *ApJS*, 99, 173
- Leitherer, C., Vacca, W. D., Conti, P. S., Filippenko, A. V., Robert, C., & Sargent, W. L. W. 1996, *ApJ*, 465, 717
- Lilly, S.J., Le Fèvre, O., Crampton, D., Hammer, F., & Tresse, L. 1995a, *ApJ*, 455, 50
- Lilly, S.J., Tresse, L., Hammer, F., Crampton, D., & Le Fèvre, O. 1995b, *ApJ*, 455, 108
- Lu, L., Sargent, W.L.W., & Barlow, T.A. 1997, *ApJ*, 484, 131
- Lu, L., Sargent, W.L.W., Barlow, T.A., Churchill, C.W., & Vogt, S.S. 1996, *ApJS*, 107, 475
- Madau, P. 1995, *ApJ*, 441, 18
- Madau, P. 1997, in *The Hubble Deep Field*, eds. M. Livio, S.M. Fall, & P. Madau (Cambridge: Cambridge University Press), in press
- Madau, P., & Shull, J.M. 1996, *ApJ*, 457, 551
- Meier, D.L., & Terlevich, R. 1981, *ApJ*, 246, L109
- Meurer, G.R., Heckman, T.M., Lehnert, M.D., Leitherer, C., & Lowenthal, J. 1997, *AJ*, 114, 54
- Meurer, G.R., Heckman, T.M., Leitherer, C., Kinney, A., Robert, C., & Garnett, D.R. 1995, *AJ*, 110, 2665.
- Miralda-Escudé, J., & Rees, M.J. 1997, *ApJ*, 478, L57
- Mo, H.J., & White, S.D.M. 1996, *MNRAS*, 282, 347
- Neufeld, D.A. 1991, *ApJ*, 370, L85
- Pettini, M., et al. 1997, in preparation
- Pettini, M., Hunstead, R.W., Smith, L.J., & King, D.L. 1995, in *QSO Absorption Lines*, ed. G. Meylan (Heidelberg: Springer), 71
- Pettini, M., Smith, L.J., King, D.L., & Hunstead, R.W. 1997, *ApJ*, 486, in press

- Rees, M.J., & Miralda-Escudé, J. 1997, ApJ, submitted
- Seitz, S., Saglia, R.P., Bender, R., Hopp, U., Belloni, P., & Ziegler, B. 1997, MNRAS, (astro-ph/9706023)
- Steidel, C.C., Adelberger, K.L., Dickinson, M., Giavalisco, M., Pettini, M., & Kellogg, M. 1997, ApJ, submitted
- Steidel, C.C., Giavalisco, M., Pettini, M., Dickinson, M., & Adelberger, K.L. 1996, ApJ, 462, L17
- Steidel, C.C., & Hamilton 1992, AJ, 104, 941
- Steidel, C.C., & Hamilton 1993, AJ, 105, 2017
- Steidel, C.C., Pettini, M., & Hamilton, D. 1995, AJ, 110, 2519
- Thompson, D., Djorgovski, S., & Trauger, J. 1995, AJ, 110, 963
- Tresse, L., & Maddox, S.J. 1997, MNRAS, submitted
- Valls-Gabaud, D. 1993, ApJ, 419, 7
- Williams, L.L.R., & Lewis, G.F. 1997, MNRAS, 281, L35
- Yee, H.K.C., Ellingson, E., Bechtold, J., Carlberg, R.G., & Cuillandre, J.C. 1996, AJ, 111, 1883